Response to Reader comments of j.carbon.2018.04.081

We appreciate the Reader for sustained concerns to our publications. We welcome all critical discussions, rather than subjective assumption of scientific misconduct, to get to the truth of developing new material and make progress in related topics, especially synthetic chemistry.

Actually, we received the same comments transferred from the editor of *Journal of Materials Chemistry A* before. We have offered a detailed response and provided original experimental data, and finally got an objective appraisal as "**it is clear that the data reported in these papers are origin**" from an independent expert.

1. Firmly deny the accusation of scientific misconduct

First of all, we deny the irresponsible accusation that "the results have been fabricated, and the authors committed scientific misconduct". **All data presented in our papers are origin without any artificial manipulation and concealment, and all published results are subject to rigorous peer review.**

The origin data of XRD, TEM/HRTEM images, SAED patterns, XPS spectra, and FT-IR spectra of the Carbon (*Carbon* 2018, *136*, 248-254) and JMCA papers (*J. Mater. Chem. A*, 2019, *7*, 5981-5990; *J. Mater. Chem. A*, 2018, *6*, 20947-20955) are provided online as follows:

Online address: https://pan.baidu.com/s/1mdJCQDHMRMcS5FcLdphMdQ

Password: upw5

These raw HRTEM images and corresponding SAED patterns contain clear scale bars and accurate test time. **These images are taken continuously from different regions**

of one single sample and there is no deliberate selection for publication. We firmly declare no scientific misconduct in our papers. Everyone including the Reader is welcome to download and strictly check these raw data.

2. Discovery of γ-graphyne from hexabromobenzene and CaC_2

It should be accepted that all researches are based on the previous reports. The synthesis of graphyne, a novel sp^2-sp carbon material, from hexabromobenzene ($PhBr_6$) and CaC_2 also refers to a series of previous works. For this, it is not without precedent. As early as in 2011, Wacharasindhu *et. al.* [1] had reported that CaC_2 could react with iodobenzene to connect benzene rings by C≡C linkages (Figure R1a). In 2017, Li *et. al.* synthesized a series of alkynyl carbon materials from CaC_2 and polyhalogenated hydrocarbons by interfacial mechanochemical reactions [2]. Subsequently, they reported efficient destruction of hexachlorobenzene (PhX_6, X= Cl, Br) by CaC_2 through the mechanochemical reaction in a planetary ball mill [3-4]. As shown in Figure R1b and R1c, they proposed a possible sp^2-sp carbon framework of the generated carbonaceous product, which is precisely what we studied on. In other words, Li *et. al.* paid their attention to the remove of halogen from the organic reactants in term of environmental science; and our contribution is pronouncing the carbonaceous product as γ-graphyne and verifying its semiconductor characteristic (*Carbon*, 2018, *136*, 248-254; *J. Mater. Chem. A*, 2018, *6*, 20947-20955), as well as Li^+/Na^+ storage properties (*Small*, 2019, *15*, 1804710; *Small*, 2020, *16*, 1907365). Li *et. al.*, independent researchers, also reported the mechanochemical synthesis of naphyne (alkynyl-linked naphthyl carbon skeleton) using CaC_2 and perchloronaphthalene precursors [5], following the same mechanism to that of mechanochemical synthesizing γ-graphyne.

γ-Graphyne is a new material with little referenced experimental data. What we can refer to is the studies of graphdiyne published before 2017. The graphdiyne, connecting adjacent benzene ring by two alkynyl linkages, has a similar molecular structure to γ-graphyne. The characterizations of as-prepared products in our work, supporting semiconductor characteristic and a higher Li^+ storage capacity than that of graphite or graphene anode, made us of confidence to identify a novel carbon material. We reported our new findings, to the best of our knowledge at that time, all based on raw characterization and measurement results without any scientific misconduct. Indeed, we were not aware of some issues in our early works, such as ignoring the existence of carbonaceous impurities and misleading assignment of X-ray diffraction peaks and SAED crystal indices (vide infra), as pointed out by the Reader. The purity problem has been recognized in our latest research [6] and ongoing work.

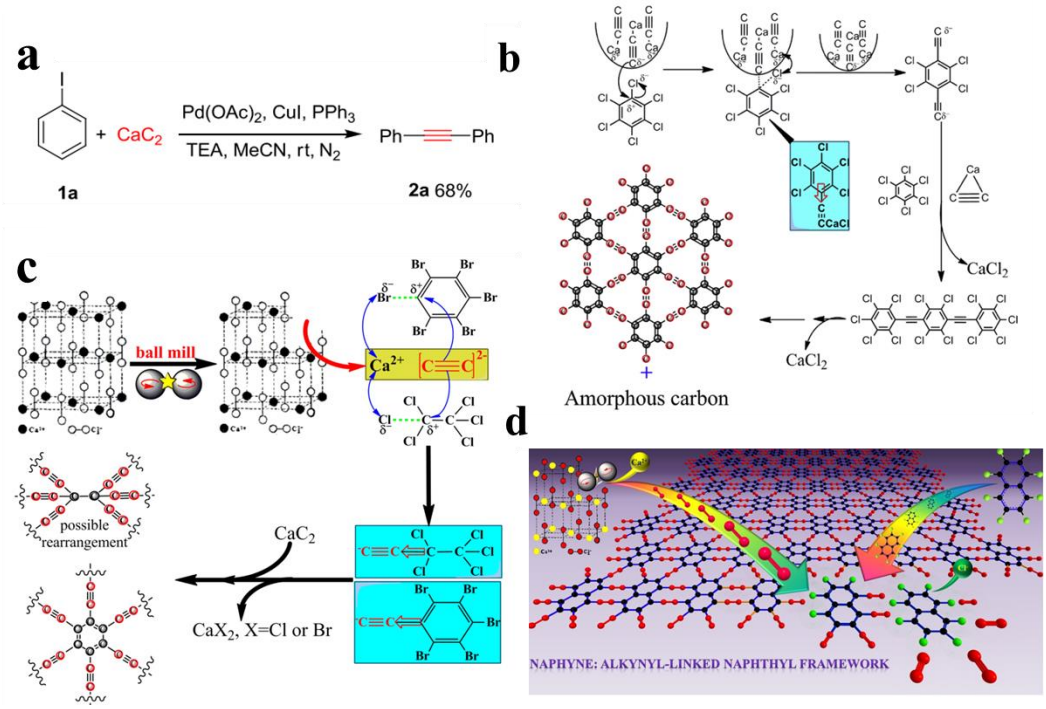

Figure R1 (a) Scheme 2 in *Tetrahedron*, 2011, *67*, 8177-8182. (b) Figure 9 in *Chemosphere*, 2017, *166*, 275-280. (c) Figure 1 in *SN Applied Sciences*, 2019, *1*, 195. (d) TOC graphic in *ACS Applied Materials & Interfaces*, 2020, *12*, 33076-33082.

2.1 Excessive amount of CaC_2 is well considered

As shown in the published carbon paper, 3.0 g $PhBr_6$ (M =551.4 g mol^{-1}, i.e. 0.00544 mol), 2.0 g CaC_2 (98%, M = 64.1 g mol^{-1}, i.e. 0.03058 mol) were used in a typical procedure, i.e. 5.62 equivalents of CaC_2 for every equivalent of $PhBr_6$. In this reaction, one-mole $PhBr_6$ consumes only three moles of CaC_2 in stoichiometry. The excessive amount of CaC_2 is well considered.

2.2 The trace water in commercial absolute ethanol

We agree with the Reader that commercial absolute ethanol (AR) still contains trace water, but the actual water content is only around 600 ppm (determined by Karl Fischer volumetric titrimetry). Thus, the total amount of trace water in the system is roughly 1.17 mmol. The feed content of CaC_2 is 30.6 mmol so that the equivalents of H_2O for every equivalent of CaC_2 is as low as 0.038. It is well known that CaC_2 can react with H_2O spontaneously ($CaC_2 + 2H_2O \rightarrow Ca(OH)_2 + C_2H_2\uparrow$), thus CaC_2 is a widely used water-removing additive in chemical reactions [7]. It is easy to remove the trace water in ethanol by excess CaC_2 before undergoing mechanochemical process.

2.3 The effect of ethanol solvent

Solvent-free is never regarded as the characteristic of mechanochemistry because process control agent is an important parameter in mechanochemistry. Several agents such as stearic acid, paraffin, ethanol and CCl_4 are considered as the widely-used process control agents, as pressed in the book of “Mechanochemistry of Materials” (Chinese Edition) [8]. Ethanol was introduced to help lowering the mechanical wear of milling balls/pots to avoid too much unexpected Fe/Fe_xO_y impurities.

Even though CaC_2 reacts directly with ethanol to generate C4-C9 alcohols byproducts

in this experiment, these alcohols should have decomposed or removed during post purifying processes. The control experiment of milling CaC_2 in ethanol without C_6Br_6 was implemented and only about 22±5 mg residue was collected after purifying, which is nearly two orders of magnitudes lower than that in experiments with C_6Br_6.

2.4 Existence of carbonaceous impurities

Under further deeply investigation, we realized the highly possible co-existence of γ-graphyne target product and carbonaceous impurities, as reported in our recent paper [6]. The carbon impurities might origin from the alkynyl homo-coupling or further carbonization of γ-graphyne because graphitic carbon is more stable than γ-graphyne in thermodynamics. Very recently, we found a competitive growth mechanism between alkynyl carbon and graphitic carbon depending on the structural symmetry of organic precursors [9]. Although the impurity problem was not recognized in our early works, it does not overturn the main conclusions of successful synthesis of novel γ-graphyne since bare graphitic carbon is impossible to present semiconductor characteristic (*Carbon*, 2018, *136*, 248-254; *J. Mater. Chem. A*, 2018, *6*, 20947-20955), high Li^+ storage capacity (*Small*, 2019, *15*, 1804710) and active Na^+ storage (*Small*, 2020, *16*, 1907365).

Up to date, effectively separating and even totally removing carbon impurities from γ-graphyne target products in this mechanochemical process is still challenging. We keep optimizing the synthesis conditions to improve the purity of γ-graphyne.

2.5 The morphology of the as-prepared sample

The gross morphology of the material described in the Carbon paper has already been discussed in our following study (*J. Mater. Chem. A*, 2019, *7*, 5981-5990). Duo to the

lack of substrate, two-dimensional carbon material trends to aggregate into bulk morphology (SEM images). After ultrasonic treatment and dispersing onto suitable substrates, it would stretch and exhibit intrinsic two-dimensional morphology (TEM & AFM images).

3. Lattice planes assignment in SAED and XRD patterns

The raw data of SAED patterns and XRD of Carbon and JMCA papers are provided online for critical checking. We only signed the lattice face and plane spacing and none of corrections were made. All scale bars were completely original.

After checking, we find that the lattice plane assignments of γ-graphyne are incorrect in our early works. In the Carbon paper, the lattice planes with the d-spacing of 0.60, 0.35 and 0.20 nm coincide with the (100), (110) and (300) lattice planes of γ-graphyne (Figure R2b), rather than (110), (211) and (422) lattice planes in the previous version. A correction would be submitted if necessary.

The d-spacing of (300) lattice plane of γ-graphyne (0.20 nm) is very close to the (100) lattice plane of graphite (0.21 nm). This is the potential reason that the Reader persists assigning SAED patterns to graphite. When carbon impurities were associated with γ-graphyne, it is not easy to distinguish γ-graphyne barely by SAED patterns. **More importantly, the innermost plots of 0.60 nm in the SAED pattern in the Carbon paper belongs to the (100) lattice plane of γ-graphyne and do not coincide with any lattice plane of graphite.**

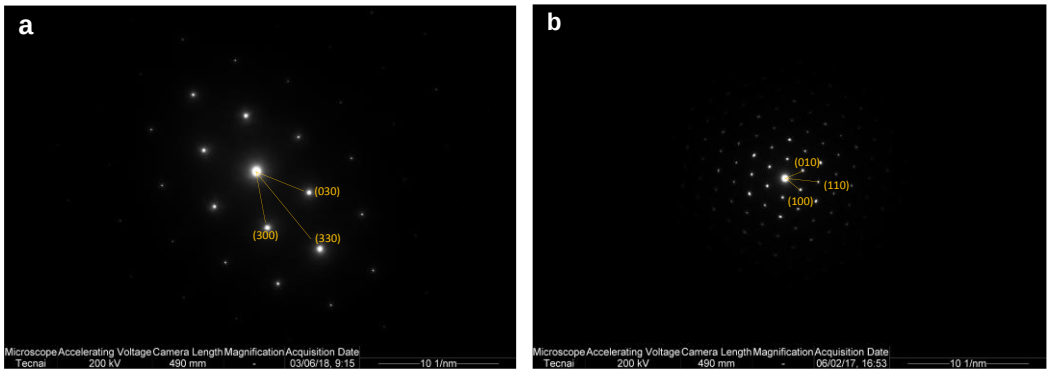

Figure R2 The revised SAED patterns in (a) the JMCA 2019 paper and (b) Carbon 2018 paper.

Besides, the assignment of X-ray diffraction peaks is misleading. As shown in Figure R3, the peaks at 25.4° (d = 0.35 nm) and 29.5° (d =0.30 nm) is indexed to (110) and (200) lattice plane of γ-graphyne. The residual peaks arise from $Ca(OH)_2$ (PDF No. 44-1481) impurities derived from CaC_2. The interference of incompletely-removed impurities was not realized adequately, leading to the incorrect assignment in our earliest work. However, our origin data still support the crystal characteristic of γ-graphyne. The d-spacings of 0.35 nm in XRD and SAED patterns correlate with each other for the (110) lattice plane of γ-graphyne. The peak intensity of (110) and (200) lattice planes of γ-graphyne indicates an AA- or AB-stacking mode [10].

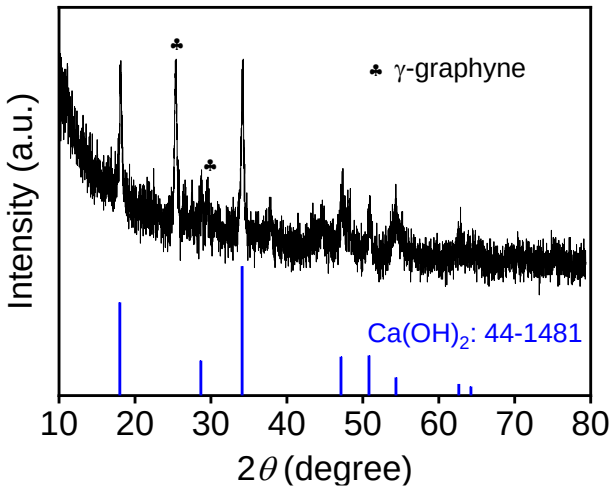

Figure R3 The XRD patterns in Carbon 2018 paper.

4. Other details on data processing

4.1 Deconvolution of XPS C1s core-level spectra

Here, the raw data (.asn file) are provided online. The XPS spectra in the Carbon paper was adjusted referring to C1s of 284.6 eV (internal standard), while that in the JMCA 2019 paper was adjusted to $Au4f_{7/2}$ of 84.0 eV (external standard). In the published edition, all peak fitting process was directly implemented on AugerScan software, one coupled with the testing system. This software does not supply any manipulation function to the background and FWHM. When opening the raw data and pressing the "Subtract Background" button, a Shirley-type background is subtracted automatically. Besides, the default fitting mode is based on 100%Gauss function with alterable FWHM.

The Reader extracted background-subtracted XPS data and carried out peak fitting, once again subtracting a Shirley-type background. The rebuild of another background will change the raw XPS data. Furthermore, the FT-IR spectra is very sensitive to C-H bond (2800–3000 cm^{-1}), but there is little C–H bond signal in the sample (Figure 2c in the JMCA 2019 paper). Thus, introducing C–H bonds in peak fitting would not be suitable, and more importantly, the assignment of C–H sp^2 (283.7 eV) and C–H sp^3 (282.7eV) is farfetched with weak support from as-cited *ref. Anal. Chem.* 2016, *88*, 6110-6114.

Considering the specific requirement of FWHM and Lorentzian/Gaussian ratio arisen from the Reader, the original data were refitted by another third-party software of XPSPEAK 4.1 under Shirley background, fixed FWHM, and 20% Lorentzian/Gaussian ratio (Figure R4). The updated fitting data of XPS spectra still support the conclusion that the final obtained samples compose of approximately equal amount of sp- and sp^2-hybridized carbon atoms. The detected oxygen results from the absorbed oxygen-

containing groups on the surface, which has been widely reported in γ-graphdiyne, another kind of full-carbon material [11-15]. XPS is a surface analysis technique so that the elemental environment analysis is relatively credible, but the comparison on absolute oxygen content is meaningless under various testing condition. The total chemical composition could be characterized by EDX spectra more accurately.

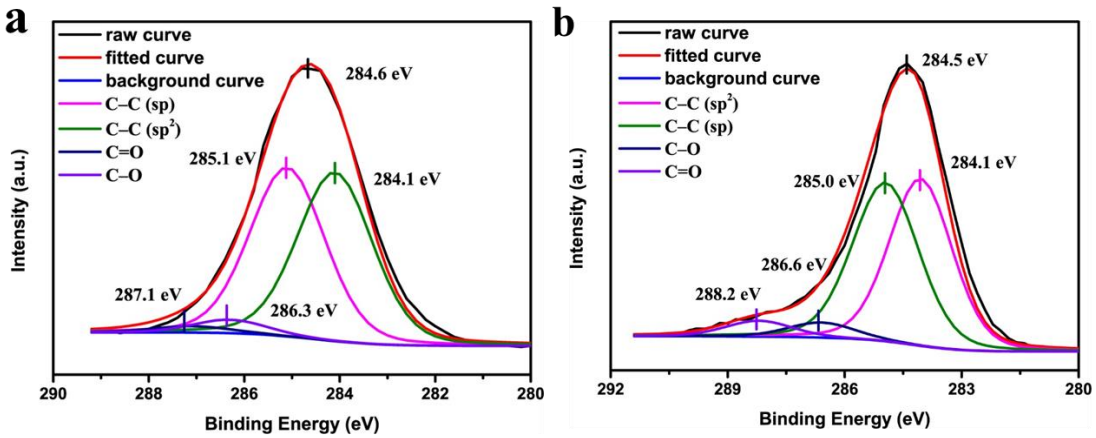

Figure R4 XPS C1s spectra of the sample in (a) *Carbon*, 2018, *136*, 248-254 and (b) *J. Mater. Chem. A*, 2019, *7*,5981-5990.

4.2 Raman shift and noise ratio

Figure R5 presents a series of published Raman spectra of graphdiyne collected from theoretical calculation [16] and experiments from different groups [11, 17 - 21]. The phenomenon of weak intensity and changeable position of Y-band (relating to alkynyl groups) is common in graphdiynes. Even for the same sample in one article, the Raman spectra will vary with different experimental conditions. The Raman shift of graphdiyne/graphyne are not as fixed as graphite. The γ-graphynes reported by our group is made by different experimental conditions (dry milling or wet milling, with or without annealing treatment, various milling speed and time, element doping and content variation, different sizes of CaC_2 precursors, and so on). Continuous

improvement of experimental conditions is being studied to decrease grinding media (such as stainless steel) and carbon impurities or to optimize defects.

Graphdiynes with high-resolution Raman signals were always grown on Cu or other specific substrate by organic synthesis, which is easy to obtain high-purity sample. Our samples were synthesized via mechanochemical method which unavoidably introduce plenty of impurities. These impurities must affect the noise ratio and the intensity of Y-band of Raman spectra. Improving the noise ratio by collecting more scans is a signal processing method, which may not be accessible for any group. FFT smoothing is also useful to decrease the noise ratio, meanwhile the raw data presents as well, which is convenient to judge whether the signal is fabricated by intuitively comparing the raw and smooth lines.

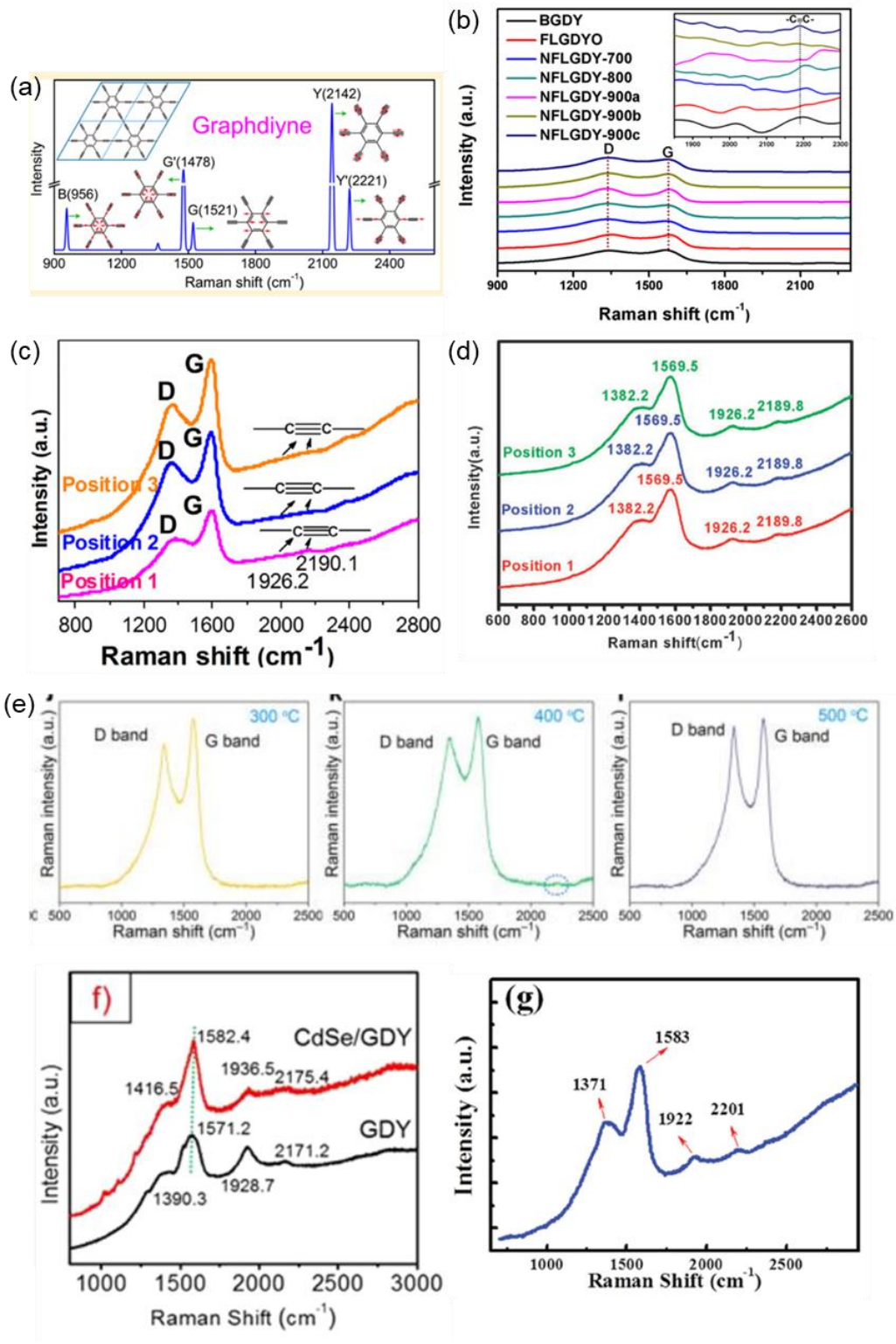

Figure R5 The published Raman spectra of graphdiyne. (a) *J. Phys. Chem. C*, 2016, *120*, 10605-10613 (theoretical spectra), (b) *Nature Chemistry*, 2018, *10*, 924-931, (c) *Nano Energy*, 2015, *11*, 481-489, (d) *Chem. Commun.*, 2010, *46*, 3256-3258, (e) *Nano Energy*, 2015, *11*, 481-489, (f) *J. Am. Chem. Soc.*, 2016, *138*, 3954−3957, and (g) *Adv. Funct. Mater.*, 2016, *26*, 5284-5289.

5. Summary

All the accusations depend on the Reader's assumption that the scale bars fabricated. But the scale bar in our publishing is original and the raw data are provided for any checking. We welcome all the discussions on the publications from readers in the world. While no material is perfect. We are still on the way to pursue the truth.

References

[1] Chuentragool, P., Vongnam, K., Rashatasakhon, P., Sukwattanasinitt, M., Wacharasindhu, S. Calcium carbide as a cost-effective starting material for symmetrical diarylethynes via Pd-catalyzed coupling reaction. Tetrahedron, 2011, 67(42), 8177-8182.

[2] Li, Y., Liu, Q., Li, W., Meng, H., Lu, Y., Li, C. Synthesis and supercapacitor application of alkynyl carbon materials derived from CaC_2 and polyhalogenated hydrocarbons by interfacial mechanochemical reactions. ACS Applied Materials & Interfaces, 2017, 9(4), 3895-3901.

[3] Li, Y., Liu, Q., Li, W., Lu, Y., Meng, H., Li, C. Efficient destruction of hexachlorobenzene by calcium carbide through mechanochemical reaction in a planetary ball mill. Chemosphere, 2017, 166, 275-280.

[4] Li, Y., Li, Y., He, X., Gu, J., Yu, M., Li, W., Li, C. Efficient synthesis of alkynyl carbon materials derived from CaC_2 through solvent-free mechanochemical strategy for supercapacitors. SN Applied Sciences, 2019, 1(2), 195.

[5] Li, Y., Li, Y., Lin, P., Gu, J., He, X., Yu, M., Wang, X., Liu, C., Li, C. Architecture and electrochemical performance of alkynyl-linked naphthyl carbon skeleton: naphyne. ACS Applied Materials & Interfaces, 2020, 12(29), 33076-33082.

[6] Chen, Y., Li, Q., Wang, W., Lu, Y., He, C., Qiu, D., Cui, X. Mechanochemical constructing ordered rhombic channels in graphyne analogues for rapid

potassium-ion storage. 2D Materials, 2021, 8(4), 044012.

[7] Fu, R., Li Z., Gao, L., Directly synthesis of organic compounds using calcium carbide as the ethylenene source. Progress in Chemistry, 2019, 31(9), 1303-1313

[8] Yang, H., Mechanochemistry of Materials. pp. 8, Science Press, Beijing 2010. ISBN 978-7-03-026290-5

[9] Lu, Y., Chen, Y., Li, Q., Hao, Z., Wang, L., Qiu, D., He, C., Wang, M., Cui, X. Carbon 2022, 194, 274-281

[10] Hu, Y., Wu, C., Pan, Q., Jin, Y., Lyu, R., Martinez, V., Huang, S., Wu, J., Wayment, L. J., Clark, N. A., Raschke, M. B., Zhao, Y., Zhang, W. Synthesis of γ-graphyne using dynamic covalent chemistry. Nature Synthesis, 2022, 1, 449-454.

[11] He, J., Wang, N., Cui, Z., Du, H., Fu, L., Huang, C., Yang, Z., Shen X., Yi, Y., Tu Z. Li, Y. Hydrogen substituted graphdiyne as carbon-rich flexible electrode for lithium and sodium ion batteries. Nature Communications, 2017, 8(1), 1-11.

[12] Zhao, Y., Wan, J., Yao, H., Zhang, L., Lin, K., Wang, L., Yang, N., Liu, D., Song, L., Zhu, J. and Gu, L., Liu, L., Zhao, H., Li, Y. & Wang, D. Few-layer graphdiyne doped with sp-hybridized nitrogen atoms at acetylenic sites for oxygen reduction electrocatalysis. Nature Chemistry, 2018, 10(9), 924-931.

[13] Zhou, J., Gao, X., Liu, R., Xie, Z., Yang, J., Zhang, S., Zhang, G., Liu, H., Li, Y., Zhang, J. Liu, Z., Synthesis of graphdiyne nanowalls using acetylenic coupling reaction. Journal of the American Chemical Society, 2015, 137(24), 7596-7599.

[14] Wang, N., Li, X., Tu, Z., Zhao, F., He, J., Guan, Z., Huang, C., Yi, Y. Li, Y. Synthesis and electronic structure of boron-graphdiyne with an sp-hybridized carbon skeleton and its application in sodium storage. Angewandte Chemie, 2018, 130(15), 4032-4037.

[15] Li, J., Xie, Z., Xiong, Y., Li, Z., Huang, Q., Zhang, S., Zhou, J., Liu, R., Gao, X., Chen, C. Tong, L. Architecture of β‐graphdiyne-containing thin film using modified glaser-hay coupling reaction for enhanced photocatalytic property of TiO_2. Advanced Materials, 2017, 29(19), 1700421.

[16] Zhang, S., Wang, J., Li, Z., Zhao, R., Tong, L., Liu, Z., Zhang, Jin., Liu, Z. Raman spectra and corresponding strain effects in graphyne and graphdiyne. The Journal

of Physical Chemistry C, 2016, 120(19), 10605-10613.

[17] Huang, C., Zhang, S., Liu, H., Li, Y., Cui, G., & Li, Y. Graphdiyne for high capacity and long-life lithium storage. Nano Energy, 2015, 11, 481-489.

[18] Li, G., Li, Y., Liu, H., Guo, Y., Li, Y., & Zhu, D. Architecture of graphdiyne nanoscale films. Chemical Communications, 2010, 46(19), 3256-3258.

[19] Huang, C., Zhang, S., Liu, H., Li, Y., Cui, G., & Li, Y. Graphdiyne for high capacity and long-life lithium storage. Nano Energy, 2015, 11, 481-489.

[20] Li, J., Gao, X., Liu, B., Feng, Q., Li, X. B., Huang, M., Liu, Z., Zhang, J., Tung, C., Wu, L. Graphdiyne: a metal-free material as hole transfer layer to fabricate quantum dot-sensitized photocathodes for hydrogen production. Journal of the American Chemical Society, 2016, 138(12), 3954-3957.

[21] Jin, Z., Yuan, M., Li, H., Yang, H., Zhou, Q., Liu, H., Lan, X., Liu, M., Wang, J., Sargent, E., Li, Y. Graphdiyne: An efficient hole transporter for stable high-performance colloidal quantum dot solar cells. Advanced Functional Materials, 2016, 26(29), 5284-5289.